Quantitative analysis of extracellular vesicle uptake and fusion with recipient cells

Hisaaki Hirose,[†§]* Yusuke Hirai, [†§] Michihito Sasaki,[‡] Hirofumi Sawa,[‡] Shiroh Futaki[†]*

[†]Institute for Chemical Research, Kyoto University, Uji, Kyoto 611-0011, Japan.

[‡]Division of Molecular Pathobiology, International Institute for Zoonosis Control, Hokkaido University, Sapporo, Hokkaido 001-0020, Japan

[§]These authors contributed equally.

*Corresponding Authors

Tel: +81-774-38-3210. Fax: +81-774-32-3038.

E-mail: hirose.hisaaki.5m@kyoto-u.ac.jp, futaki@scl.kyoto-u.ac.jp

Abstract

In precision medicine, extracellular vesicles (EVs) are promising intracellular drug delivery vehicles. The development of a quantitative analysis approach will provide valuable information from the perspective of cell biology and system design for drug delivery. Previous studies have reported quantitative methods to analyze the relative uptake or fusion of EVs to recipient cells. However, relatively few methods have enabled the simultaneous evaluation of the "number" of EVs taken up by recipient cells and those that fuse with cellular membranes. In this study, we report a simple quantitative method based on the NanoBiT system to quantify the uptake and fusion of small and large EVs (sEVs and lEVs, respectively). We assessed the abundance of these two subtypes of EVs and determined that lEVs may be more effective vehicles for transporting cargo to recipient cells. The results also indicated that both sEVs and lEVs have very low fusogenic activity, which can be improved in the presence of a fusogenic protein.

Introduction

Almost all cell types release extracellular vesicles (EVs) containing proteins and nucleic acids, such as microRNAs (miRNAs), which play critical roles in cell-cell communication.[1] Previous studies have reported that cargo proteins and nucleic acids of EVs alter gene expression and recipient cellular functioning.[2,3,4] Thus, EVs are expected to be effective intracellular drug delivery vehicles.[5] It is believed that membrane fusion between EVs and recipient cells is necessary to release EV cargos into recipient cells before their bioactivity can be exhibited. Recent research suggests that EVs are endocytosed by recipient cells and fuse to their endosomal membranes (**[i]** and **[ii]** in Fig. 1A, respectively).[6] Nonetheless, it has also been suggested that the efficiency of the fusion is low.[7,8,9]

Evaluating the specific mechanisms underlying endocytic uptake and membrane fusion of EVs in recipient cells is vital for comprehending their cell biological significance and therapeutic applications.[10] Quantifying the fractions of EVs that fuse with endosomal membranes (**[ii]** in Fig. 1A) is key for evaluating the delivery efficacy of EV cargos. However, information on the total amount of EV uptake (**[i]** + **[ii]** in Fig. 1A) is equally crucial for understanding the endocytic EV uptake mechanisms and intracellular delivery kinetics. Although lipophilic dyes, fluorescent proteins, and luciferases have been used in numerous approaches for the evaluation of total endocytosed EVs (**[i]** + **[ii]** in Fig. 1A),[11,12,13] methods to assess the membrane fusion of EVs (**[ii]** in Fig. 1A) in recipient cells remain limited. Joshi et al. reported an assay for monitoring the membrane fusion between EVs and recipient cells. They used EVs in which GFP was tagged at the interior of the EV membrane; and recipient cells overexpressing anti-GFP fluobody.[14] The membrane fusion led to the interaction between GFP and anti-GFP fluobody, and thus could be detected by analyzing

GFP/fluobody double-positive fluorescence signals. In another approach, Somiya and Kuroda reported a quantification assay for the fusion of EVs with recipient cell membranes, using a split nanoluciferase system.[8] While these approaches allow the assessment of EV membrane fusion, it is challenging to simultaneously compare the membrane fusion efficiency with total EVs taken up by recipient cells. Additionally, these approaches are used to evaluate the relative fusion efficiency of EVs, although quantification based on the "numbers" of EVs would provide more insight. The development of quantitative methods for analyzing the amount of internalized and fused EVs will aid in elucidating the intracellular fate and delivery efficiency of diverse EVs produced from distinct cell types. Additionally, quantitative analysis can identify molecules (such as proteins, peptides, and small compounds) that enhance cellular uptake and/or membrane fusion for developing more sophisticated and efficient EV-based drug delivery strategies.

In this study, we aimed to develop a system for quantifying "the total number of EVs taken up by cells via endocytosis" (**[i]** + **[ii]** in Fig. 1A) and "the number of EVs that fuse with endosomal membranes of recipient cells" to release their contents into the cytosol (**[ii]** in Fig. 1A). For this purpose, we used the NanoBiT system, which is a split nanoluciferase (Nluc) system (Fig. 1B).[15] The split Nluc consists of an 18 kDa large subunit (LgBiT) and a small 11-mer peptide fragment (HiBiT). The NanoBiT system permits the sensitive luminescent detection of a HiBiT-tagged protein of interest in the presence of a substrate (furimazine) because the HiBiT-tag spontaneously binds to the complementary LgBiT with high affinity (K_d = 0.7 nM). EVs are subdivided into ectosomes/microvesicles (100–1000 nm in diameter) and exosomes (50–150 nm in diameter).[10] Considering that these classes of EVs may differ in intracellular fates, cellular uptake efficiencies, and membrane fusion, we

applied our quantification system to EVs composed primarily of microvesicles (designated as large EVs, lEVs) and exosomes (designated as small EVs, sEVs), to determine the possible differences.

Results and Discussion

Differentiating cellular uptake of EVs from the amount of EVs fused with recipient cells

EVs with the HiBiT peptide tag on the luminal side of the membrane were generated to assess EV uptake and fusion with recipient cells expressing LgBiT (Fig. 1B). For this purpose, we created a plasmid encoding the HiBiT peptide fused to the C-terminus of CD63, a tetraspanin membrane protein (CD63-HiBiT). Numerous studies have reported fusing proteins of interest with CD63, one of the most common EV marker proteins, to incorporate them into EVs.[16,17,18,19,20] Then, we established a single clone of U2OS cells that stably expressed CD63-HiBiT and confirmed the presence of the HiBiT peptide in both the cell lysates and the isolated EVs (Fig. S1). We also established A549 cells stably expressing LgBiT (A549-LgBiT cells) as recipient cells, as previously reported.[21] The total cellular uptake of EVs (corresponding to **[i]** + **[ii]** in Fig. 1A) was distinguished from the fused EVs in recipient cells (corresponding to **[ii]** in Fig. 1A) by performing two assays: namely cell lysis assay (yellow line in Fig. 1B) and live cell assay (green line in Fig. 1B). The cell lysis assay, which involves lysis of both endosome and EV membranes and allows for quantification of the binding of EV-derived CD63-HiBiT to cellular LgBiT, can quantify the total cellular uptake of EVs by recipient cells. In contrast, the absence of detergent in the live cell experiment did not affect these membranes. Consequently, the HiBiT peptides in EVs that have not fused with the recipient cell membrane cannot bind to LgBiT in those cells, whereas only the HiBiT peptide exposed to the cytosol as a result of membrane fusion can bind to LgBiT. In this investigation, we aimed to develop a system that quantifies the number of EVs taken up by and fused with recipient cells, which is distinct from the objectives of the study by

Somiya and Kuroda, who employed a similar split-luciferase-based technique to evaluate EV cargo release into recipient cells.[8]

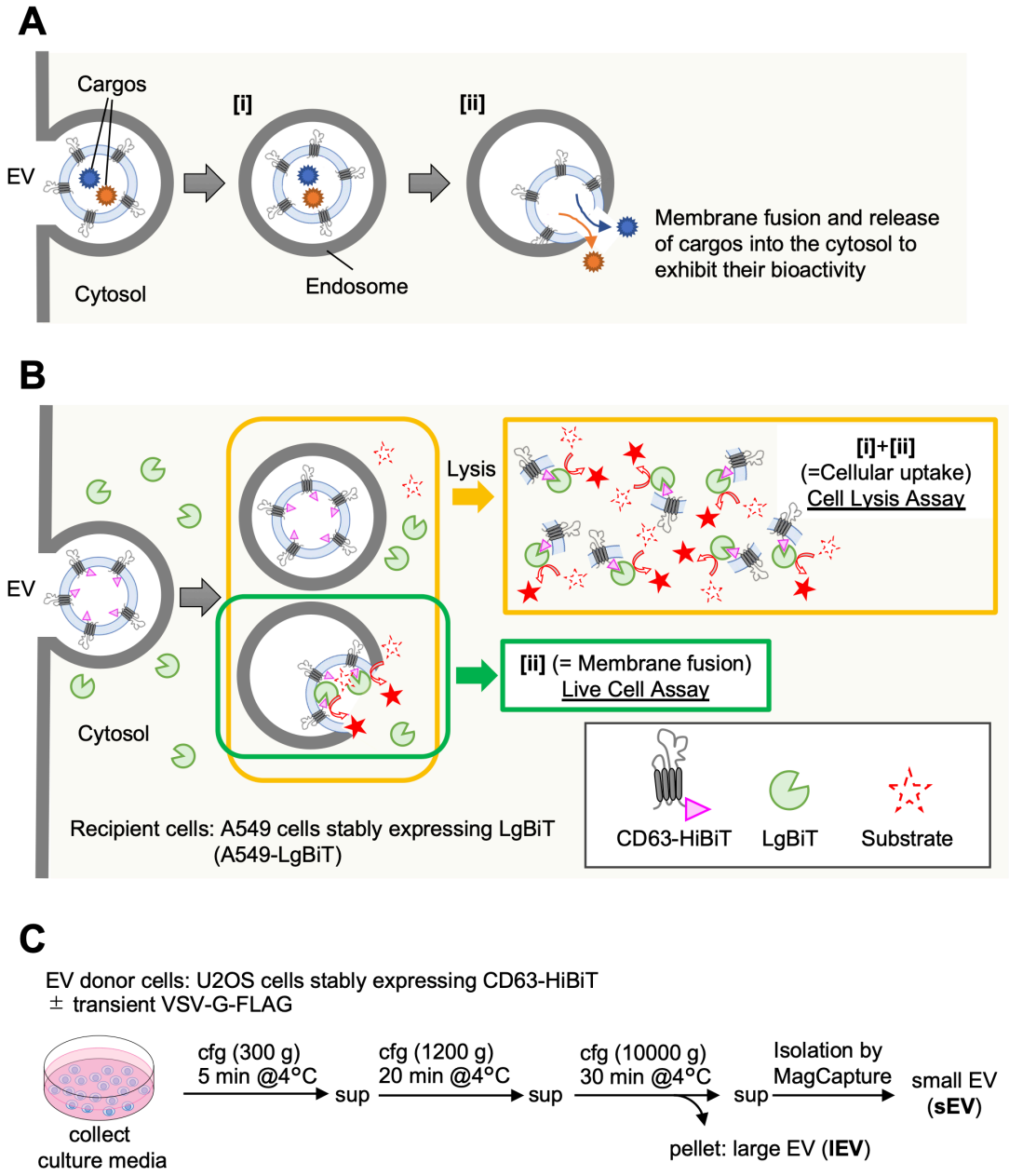

Fig. 1 Scheme illustrating the concept of the study and isolation of EVs. Prior to obtaining cargo bioactivities, (A) EVs are taken up by cells, encapsulated in their vesicular compartment (i.e., endosome) **[i]**, and subsequently fused with the endosomal membrane to release the cargos into the cytosol **[ii]**. (B) Quantification of total uptake and membrane fusion of EVs using the NanoBiT system. In this study, "Cellular uptake" of EVs is defined to include both EVs encapsulated in endosomes **[i]** and those fused with endosomal membranes **[ii]**. (C) Isolation of sEVs and lEVs. EVs, extracellular vesicles; sEVs, small extracellular vesicles; lEVs, large extracellular vesicles.

Characterization of EV subtypes

According to their biogenesis, EVs are subcategorized into ectosomes/microvesicles and exosomes.[22] Ectosomes or microvesicles are vesicles of varying sizes (100–1000 nm in diameter) pinched off from the plasma membrane.[23] Exosomes (50–150 nm in diameter) are released by exocytosis of multivesicular bodies (MVBs).[22] These classes of EVs may have distinct cellular uptake pathways and intracellular fates due to differences in vesicle sizes and EV composition (such as membrane lipids and surface displayed proteins and sugars). Considering the paucity of information in this context, we investigated whether the two classes of EVs have different cellular uptake mechanisms and intracellular fates based on EV quantity. Although it is challenging to completely differentiate microvesicles from exosomes, EVs can be effectively separated and isolated based on their sizes and centrifugation speeds.[24] The supernatant obtained from sequential centrifugation at 300 × *g* and 1,200 × *g* was subjected to further centrifugation at 10,000 × *g* to obtain pellets primarily comprising microvesicles (*i.e.,* lEVs) (Fig. 1C). The supernatant was further treated with MagCapture beads,[25] allowing Ca^{2+}-dependent preferential exosome purification through interaction with the phosphatidylserine displayed on their surfaces, yielding exosome-rich fractions (*i.e.,* sEVs).

We characterized the isolated sEVs and lEVs derived from U2OS cells stably expressing CD63-HiBiT by western blotting and the nano tracking analysis (NTA) system (Fig. S2 and S3). Western blot analysis showed that both sEVs and lEVs contain the EV markers CD63 and CD9 (Fig. S2A). In addition, Syntenin1 and Annexin A1 have been identified as markers of exosomes and microvesicles, respectively.[26,27] Western blot analysis revealed that the sEV fraction contained high levels of Syntenin1 and low

levels of Annexin A1, whereas the lEV fraction contained high levels of Annexin A1 and low levels of Syntenin1 (Fig. S2A). These findings validated the characterization of sEVs and lEVs. In addition, we determined the presence of CD63-HiBiT in sEVs and lEVs using the HiBiT detection system (Fig. S2B and S2C).

Analysis of endocytic uptake pathways of EVs

Before analyzing the mechanisms underlying endocytic uptake and fusion of EVs, we verified that the cell lysis assay quantifies the total uptake of both sEVs and lEVs. The assay also examined their cellular uptake mechanisms into A549-LgBiT cells (Fig. 2A and 2B). Varying amounts of isolated sEVs and lEVs were lysed and combined with the lysates of A549-LgBiT cells in each experiment to generate a luminescence standard curve as a function of EV protein content. A linear relationship between luminescence and the amount of sEVs/lEVs in the range of 0–1000 ng was established (Fig. S4), indicating that the luminescence intensities accurately represent the quantity of EVs. The sEVs or lEVs (300 ng as total protein) were incubated with A549-LgBiT cells for 2, 4, and 24 h. The results showed a time-dependent increase in cellular uptake of both sEVs and lEVs up to 24 h. This method enabled us to quantify the amount of cellular uptake at each time point, *e.g.*, ~ 4.5% and ~ 25% of incubated sEVs and lEVs were internalized after 24 h, respectively. Our results suggest that the cellular uptake efficiency of lEVs is higher than that of sEVs. Inhibitor investigations have revealed that clathrin-mediated endocytosis and macropinocytosis may be involved in EV uptake by cells.[8, 28] Using our system, we confirmed similar inhibitory effects. Cellular uptake was markedly inhibited when both sEVs and lEVs were incubated with A549-LgBiT cells at 4 °C for 4 h, suggesting that the EVs were internalized into the cells via energy-dependent endocytosis pathways. The cellular uptake of sEVs and lEVs was significantly inhibited

by clathrin-mediated endocytosis inhibitors, Pitstop2 and chlorpromazine (CPZ), and the macropinocytosis inhibitors, 5-(*N*-ethyl-*N*-isopropyl) amiloride (EIPA), and wortmannin. However, the caveolae-dependent endocytosis inhibitor Nystatin did not affect cellular uptake.

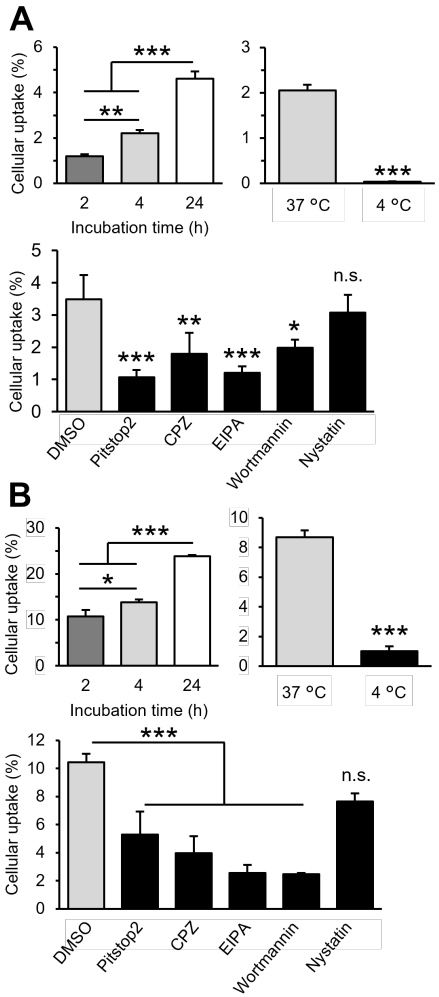

Fig. 2 Evaluation of EV uptake into A549-LgBiT cells. (A) sEV uptake data. (B) lEV uptake data. The results are presented as mean ± standard deviation (SD) (n = 3). $^{**}P < 0.01$; $^{***}P < 0.001$ (one-way analysis of variance [ANOVA] followed by Tukey-Kramer's honestly-significant difference test for time-course uptake data, ANOVA followed by unpaired *t*-test for temperature-dependent uptake data, and Dunnett's post-hoc test vs. dimethyl sulfoxide (DMSO; vehicle control) for endocytosis inhibiting data). EVs, extracellular vesicles; sEVs, small extracellular vesicles; lEVs, large extracellular vesicles.

Quantitative analysis of the number of EVs taken up by recipient cells

After confirming the fidelity of EVs, we conducted a particle number-based quantitative analysis of the modes of cellular uptake for both sEVs and lEVs. A549-LgBiT cells (9×10^4 cells seeded one day before each experiment) were incubated with sEVs or lEVs (5×10^8 particles) for 24 h (Table 1). The numbers of EVs employed in each independent experiment were determined using the NTA system; luminescence standard curves were generated as a function of the numbers (Fig. S5B and S5C) (see the experimental procedures for details). The cells treated with EVs were lysed, and numbers of sEVs and lEVs taken up by the cells were obtained using the luciferase activity. The cell lysis assay revealed that ~6% of total sEVs and ~18% of total lEVs were internalized by A549-LgBiT cells in 24 h, indicating that ~90 sEV particles and ~270 lEV particles were internalized per cell (Table 2, sEVs and lEVs, total cellular uptake). The EVs taken up by the cells were successfully quantified. This quantification also demonstrated that the lEVs were preferentially taken up by the cells.

Quantitative analysis of the number of EVs fused with recipient cells

From a drug delivery perspective, it is crucial to realize the actual ratio of EVs fused with endosomal membranes to release their cargos into the cytosol of recipient cells. Because the tetraspanin-tagged HiBiT peptide in the cytosol of recipient cells should reconstitute Nluc with LgBiT to exert luciferase activity, EVs fused with endosomal membranes could be detected in live cell luminescence assays performed without cell lysis. However, since the same amount of reconstituted Nluc is affected differently by the differences between the lysis and the live cell assays (for example, the presence and absence of a detergent), corrections were needed for luminescent intensities obtained in

all the live cell assays. [29] We obtained the correction factor (0.72) based on a previously reported method[29] (Fig. S5A).

Contrary to our expectations, the live cell assay revealed that the endogenous fusogenic activity of EVs is significantly lower than the efficacy observed in the cellular uptake (Table 2, membrane fusion). No fusion was detected for sEVs under the described experimental conditions (Table 2, sEVs). Even in the case of lEVs, only ~0.02% of the total administered lEVs fused with the recipient cells (Table 2, lEVs). Our results for sEVs are consistent with those of a previous study suggesting no membrane fusion of EVs.[8] However, our method detected a small portion of membrane fusion between lEVs and recipient cells, indicating that lEVs may have detectable fusogenic activity. It has been reported that decorating EVs with the fusogenic envelope glycoprotein G of the vesicular stomatitis virus (VSV-G) significantly improved their fusion activity.[8] VSV-G have been employed to promote membrane fusion in virus/EV-based delivery systems.[30,31] Thus, we applied our quantification system to evaluate the promotion effect and determine possible variations in this effect for sEVs and lEVs. sEVs and lEVs were isolated from U2OS-CD63-HiBiT cells transiently expressing FLAG-tagged VSV-G (VSV-G-FLAG), as described above. The western blotting analysis confirmed the presence of VSV-G-FLAG in these EVs (Fig. S2B and S2C). The sizes of isolated sEVs and lEVs were comparable to those without VSV-G-FLAG expression (Fig. S3). The presence of VSV-G-FLAG significantly increased the efficiency of membrane fusion of sEVs and lEVs to the recipient cells (*i.e.*, ~3% and ~7% of total sEVs and lEVs, respectively) (Table 2, sEVs with VSV-G, lEVs with VSV-G), with ~40 sEV particles and ~100 lEV particles fusing per cell. These results emphasized the potential superiority of lEVs as intracellular delivery vehicles. Our results suggest low fusion efficacy of both sEVs and lEVs regarding fusion with recipient cells in the absence of a fusogenic protein.

However, successful transfer of cargos, including miRNAs encapsulated in EVs, to the recipient cells has been reported. [32,33,34,35] Therefore, further research is needed to clarify the reasons for this observation. One possible explanation for this discrepancy is that membrane fusion events are too transient to be detected by the reconstitution of cytosolic LgBiT with HiBiT-tagged membrane proteins in EVs. Other diverse EV-donor and recipient cells should be examined in the future. Another possibility is that some cargos are transferred into recipient cells via connexin 43, a gap junction protein,[36] suggesting that communication between EVs and recipient cells is possible even without canonical membrane fusion. The positive effect of VSV-G-FLAG on EV cargo delivery to recipient cells supports the idea that developing methods to enhance membrane fusion between EVs and recipient cells is necessary for applying EVs to efficient drug delivery.

Table 1 Number of cells and EVs in treatment

Cells seeded	Added EVs (particles)	Cells after treatment with EVs
9.0E+4 cells	5.0E+8 particles/well	3.4E+5 ± 1.6E+4 cells

Table 2 Summary of quantification of cellular uptake and membrane fusion of extracellular vesicles to receptor cells

EVs	Total cellular uptake		
	%	Particles	Particles/cell
sEV	6.1 ± 2.2	3.1E+7 ± 1.1E+7	92 ± 33
sEV with VSV-G	5.9 ± 2.1	3.0E+7 ± 1.1E+7	88 ± 32
IEV	18.1 ± 3.7	9.1E+7 ± 1.9E+7	271 ± 56
IEV with VSV-G	18.0 ± 5.2	9.0E+7 ± 2.6E+7	269 ± 77

EVs	Membrane fusion		
	%	Particles	Particles/cell
sEV	−0.01 ± 0.01	−8.3E+4 ± 5.8E+4	−0.2 ± 0.2
sEV with VSV-G	2.9 ± 0.2	1.5E+7 ± 0.1E+7	43 ± 3
IEV	0.02 ± 0.003	7.8E+4 ± 1.8E+4	0.2 ± 0.1
IEV with VSV-G	6.9 ± 2.3	3.5E+7 ± 1.2E+7	103 ± 35

Conclusions

Using the NanoBiT system, we established a simple and quantitative method for evaluating the number of EVs internalized and fused with recipient cells. We evaluated the cellular uptake and membrane fusions of two EV subtypes (sEVs and lEVs) and found that the lEVs may be superior vehicles for delivering cargo to recipient cells. Our results also suggested the low fusion efficacy of both sEVs and lEVs in the absence of a fusogenic protein. The positive effect of the fusogenic protein VSV-G on the cargo delivery of EVs to recipient cells provides the baseline for developing methods to enhance EV-recipient cell membrane fusion. Overall, we established a system for estimating the cellular uptake and eventual fusion with recipient cells based on the ratio of EVs to cells. This was accomplished using NTA to quickly estimate the number of EVs and the split luciferase system to assess delivery activity. In addition, differences in the cellular uptake and fusion efficacy of sEVs and lEVs were observed. This study roughly fractionated EVs into sEVs and lEVs based on their particle sizes. However, it should be noted that each fraction of EVs should contain various types of vesicles composed of discrete protein, sugar, and lipid components; the results were an average of EVs in each subtype. This study suggested that lEVs are more efficient than sEVs in cellular uptake and fusion under the described experimental conditions. Next, it shall be crucial to identify the factors (such as particle size, surface proteins and saccharides, and lipid components) critical for the enhanced cargo delivery efficiency. Understanding these factors can deepen our knowledge of EV-mediated cellular communications and aid in establishing more advanced EV-mediated delivery systems. To this end, the results identifying the higher delivery efficiency of lEVs over sEVs are particularly noteworthy. Overall, our findings are valuable for conducting additional research to gain a more nuanced understanding of the modes of cellular uptake and intracellular fates of different

EVs and for screening reagents, peptides, and proteins that enhance cellular uptake and membrane fusion.

Experimental procedures

Materials

MagCapture Exosome Isolation Kit PS was purchased from FUJIFILM Wako Pure Chemical Corp (Osaka, Japan). Pitstop2, CPZ, EIPA, and nystatin were acquired from Sigma-Aldrich (St. Louis, MO, USA). Wortmannin was obtained from Funakoshi (Tokyo, Japan). Primers and DNA oligonucleotides were procured from Invitrogen (Carlsbad, CA, USA). Primer sequences and DNA oligonucleotides used in this study are listed in Table S1. Nano-Glo HiBiT Lytic Detection System, Nano-Glo Live Cell Assay system, and Nano-Glo HiBiT Blotting System were purchased from Promega (Madison, WA, USA). The antibodies used in this study are listed in Table S2.

Plasmid construction

Dr. Martin Fussenegger (ETH Zürich, Switzerland) generously provided the CD63-L7Ae plasmid.[10] The (GGGS)2-HiBiT coding fragment was obtained by annealing two oligonucleotides (oligo-HiBiT_Fw and oligo-HiBiT_Rv) that had been phosphorylated at their 5′-ends with T4 polynucleotide kinase (New England Biolabs). This sequence was inserted between the EcoRI and ApaI restriction enzyme sites of the CD63-L7Ae plasmid to yield CD63-(GGGS)2-HiBiT (referred to as CD63-HiBiT). The VSV-G-HiBiT plasmid was generously provided by Dr. Masaharu Somiya (Osaka University, Japan).[7] VSV-G-HiBiT plasmid was amplified by PCR using forward and reverse primers (VSV-G_Fw and VSV-G_Rv, respectively). Following that, we used NEBuilder HiFi DNA assembly master mix (New England Biolabs, Ipswich, MA, USA) to assemble a DNA duplex by annealing two oligonucleotides (oligo-FLAG_Fw and oligo-FLAG_Rv) with the amplified fragments, yielding a VSV-G-FLAG (FLAG tag:

DYKDDDDK) plasmid, according to the manufacturer's instructions. Dr. Timothy Stasevich (Colorado State University, The United States) generously provided the pHis-MCP-HaloTag plasmid.[37] To obtain the amplified DNA fragment encoding HaloTag, PCR was performed using forward and reverse primers (Halo Tag_Fw and Halo Tag_Rv, respectively). Then, the CD63-HiBiT plasmid was amplified by PCR using forward and reverse primers (HiBiT_Fw and HiBiT_Rv, respectively), and the amplified fragment encoding HaloTag was assembled with NEBuilder HiFi DNA assembly master mix according to the manufacturer's instructions.

Establishment of U2OS cells stably expressing CD63-HiBiT

U2OS cells (1.2×10^6 cells) were seeded onto a 100 mm dish and incubated for 1 day. Then, the cells were transfected with CD63-HiBiT plasmid (11 μg) complexed with Lipofectamine LTX reagent (33 μL) with PLUS reagent (11 μL) in Dulbecco's Modified Eagle's Medium (DMEM) High Glucose (HG) containing 10 % fetal bovine serum (FBS) for 3 h, washed, and incubated for 1 day. Next, the cells were treated with 1 mg/mL G418 (Fujifilm Wako) for the antibiotic selection of U2OS cells stably expressing CD63-HiBiT. Then, by limiting dilution, the established polyclonal pool of the cells was re-seeded into a 96-well plate and cultured in DMEM HG containing 10 % FBS with G418. Finally, we obtained a single clone stably expressing CD63-HiBiT (U2OS-CD63-HiBiT cells).

Establishment of A549 cells stably expressing LgBiT

As previously reported, Human Caucasian lung carcinoma (A549) cells stably expressing LgBiT (A549-LgBiT cells) were established as recipient cells.[15] The LgBiT coding region from pBiT1.1-C[TK/LgBiT] (Promega) was sub-cloned into CSII-CMV-

MCS-IRES2-Bsd (RIKEN BRC, Ibaraki, Japan) to construct CSII-CMV-LgBiT-IRES2-Bsd. A self-inactivating lentiviral vector was prepared by co-transfection with CSII-CMV-LgBiT-IRES2-Bsd and Lentiviral High Titer Packaging Mix (Takara Bio, Shiga, Japan) according to the manufacturer's instruction. A549-LgBiT cells were established by inoculation with the lentiviral vector and selected in the presence of blasticidin (20 μg/mL).

Cell culture and transfection

U2OS cells and U2OS-CD63-HiBiT cells were cultured in DMEM HG containing 10% FBS. In addition, A549-LgBiT cells were cultured in DMEM Low Glucose (LG) containing 10% FBS. Cells were grown in 100 mm dishes and incubated at 37 °C with 5% CO_2. U2OS or U2OS-CD63-HiBiT cells (1.2×10^6 cells) were seeded onto a 100 mm dish and incubated for 1 day. The cells were transfected with a plasmid (11 μg) complexed with the Lipofectamine LTX reagent (33 μL) and PLUS reagent (11 μL) in DMEM HG containing 10% FBS for 3 h. The cells were washed four times with 4 mL of Ca^{2+}- and Mg^{2+}- free PBS, *i.e.*, PBS(−) to remove the excess plasmid-LTX complexes from the dishes.

Isolation of large and small EVs (lEVs and sEVs)

The transfected or non-transfected U2OS-CD63-HiBiT cells cultured in 100 mm dishes were incubated in DMEM HG containing 10% exosome-depleted FBS (System Biosciences, Mountain View, CA, USA) for 2 days. The collected cell culture medium was centrifuged (300 × *g*, 4 °C, 5 min), and the supernatant was centrifuged twice (first: 1,200 × *g*, 4 °C, 20 min; second: 10,000 × *g*, 4 °C, 30 min) to yield the lEV fraction in pellets and sEV fraction in the

supernatant. The lEVs were resuspended in 100 μL of PBS(−). The sEV-containing supernatant was concentrated to 1 mL using an Amicon Ultra-15 100 kDa device (Merck Millipore, Darmstadt, Germany). The sEVs were isolated using a MagCapture Kit (FUJIFILM Wako) and eluted twice with 50 μL of elution buffer (~100 μL in total). The protein concentrations of the isolated EVs were determined using the Pierce BCA protein assay kit, a bicinchoninic acid (BCA) enhanced protocol (Thermo Fisher Scientific, Waltham, MA, USA).

Detection of HiBiT peptide

As described in the previous section, the proteins from isolated EVs were transferred to a PVDF membrane for western blotting. The membrane was incubated in TBST for 4-5 h at 25 °C to solubilize the HiBiT-tag. Nano-Glo HiBiT Blotting System (Promega) was used to detect the HiBiT-tag after the membrane was incubated in Nano-Glo Blotting Buffer containing LgBiT at 4 °C overnight according to the manufacturer's protocol using LAS3000 mini (FUJIFILM).

Quantification of cellular uptake of EVs into recipient cells (cell lysis assay)

The Nano-Glo HiBiT Lytic Detection System (Promega) was used to detect the reconstituted luciferase activity by internalized CD63-HiBiT to quantify the total cellular uptake of EVs. A549-LgbiT cells (9×10^4 cells/well) were seeded into a 24-well plate (Iwaki, Tokyo, Japan) in DMEM LG containing 10% FBS and incubated for 1 day at 37 °C with 5% CO_2. After washing with 500 μL of PBS(−) twice, the cells were incubated with the isolated EVs in DMEM LG containing 10% exosome-depleted FBS at the specified incubation time (2, 4, and 24 h). After the treatment, the cells were washed twice with 500 μL of PBS(−) to remove EVs outside the cells and then trypsinized with 100 μL of 0.01% trypsin in PBS(−) for 10 min at 37 °C with 5% CO_2. After adding 100 μL of DMEM LG containing 10% FBS, the cells were collected on

ice in a 1.5 mL tube. The cells were precipitated by centrifugation (800 × *g*, 4 °C, 5 min), and the supernatant was removed. The EV-treated cells were resuspended in a 50 μL mixture of PBS(−) and Opti-MEM (Thermo Fisher Scientific). Non-treated cells were resuspended in Opti-MEM containing determined amounts of EVs in PBS(−) at a final volume of 50 μL to create a calibration curve (x-axis, EV amount; y-axis, luminescence intensity). Next, the cells were mixed with 50 μL of HiBiT lytic detergent buffer containing the substrate for 10 min in a 96-well optical bottom white plate (Thermo Scientific Nunc, Rochester, NY, USA). Finally, luminescence intensity (counts per second) was measured at 25 °C using a Nivo plate reader (Perkin Elmer, Waltham, MA, USA) with an integration time of 1 s per well.

Investigation of cellular uptake mechanism of EVs into recipient cells

A cell lysis assay was conducted to investigate the uptake mechanism of EVs into A549-LgBiT cells. A549-LgBiT cells (9×10^4 cells/well) were seeded into a 24-well plate (Iwaki) in DMEM LG containing 10% FBS and incubated at 37 °C with 5% CO_2 for 1 day. Before adding EVs (300 ng as protein amount per well), cells were pre-incubated at either 4 °C or 37 °C for 30 min to inhibit energy-dependent endocytosis pathways. The cells were washed twice with 500 μL of cold or warm PBS(−) and treated with the isolated EVs in DMEM LG containing 10% exosome-depleted FBS at 4 °C or 37 °C for 4 h. Following treatment, the cells were collected, and luminescence measurements were taken as described in the cell lysis assay section. The cells were pre-incubated with Pitstop2 (15 μM), CPZ (20 μM), EIPA (20 μM), wortmannin (2 μM), Nystatin (20 μM) for 30 min in DMEM LG without FBS to examine the endocytic pathways. Dimethyl sulfoxide (DMSO) (final concentration <0.5%, v/v) was used to dissolve inhibitors and as the vehicle control. Cells were treated with isolated EVs (300 ng as total protein amount) in DMEM LG containing 10% exosome-depleted FBS in the presence of each

inhibitor for 4 h. The cells were collected, and luminescence was measured following the cell lysis assay method described before.

Determination of a correction factor between cell lysis assay and live cell assay

The reconstituted luciferase activity in A549-LgBiT cells transiently expressing HaloTag-HiBiT was detected using the Nano-Glo HiBiT Lytic Detection System (Promega) and the Nano-Glo Live Cell Assay System (Promega), respectively, to obtain a correction factor between cell lysis and live cell assay. A549-LgBiT cells (4.5×10^4 cells/well) were seeded into a 24-well plate (Iwaki) in DMEM LG containing 10% FBS and incubated for 1 day at 37 °C with 5% CO_2. After washing with 500 μL of PBS(−) twice, the cells were transfected with HaloTag-HiBiT plasmid (0, 0.01, 0.1, 1, 5, 10, 50, 100 ng/well) complexed with Lipofectamine LTX reagent (0.6 μL) with PLUS reagent (0.4 μL) in DMEM LG containing 10 % FBS for 3 h. The cells were washed with PBS(−) four times and incubated in DMEM LG containing 10% FBS for 1 day. After washing with 500 μL of PBS(−) twice, the transfected cells were trypsinized with 100 μL of 0.01% trypsin in PBS(−) for 10 min at 37 °C with 5% CO_2. After adding 100 μL of DMEM LG containing 10% FBS, the cells were collected on ice in a 1.5 mL tube. The cells were precipitated by centrifugation (800 × *g*, 4 °C, 5 min), and the supernatant was removed. The cells were then resuspended with Opti-MEM (50 μL). The cells were mixed with 50 μL of HiBiT lytic detergent buffer containing the substrate for 10 min for the cell lysis assay. For the live cell assay, the cells were mixed with 50 μL of assay reagent containing the substrate in a 96-well optical bottom white plate (Thermo Scientific Nunc). Finally, the luminescence intensity (counts per second) was measured at 25 °C using a Nivo plate reader (Perkin Elmer) with an integration time of 1 s per well. A correction factor (F, lytic/live cell)

was calculated using the slope of the calibration curves (x-axis, transfected plasmid amount; y-axis, luminescence intensity).

$$\boldsymbol{F = \frac{slope\ of\ Lytic\ assay}{slope\ of\ Live\ Cell\ assay} = 0.72}$$

Quantification of membrane fusion of EVs with recipient cells (live cell assay)

The Nano-Glo Live Cell Assay System (Promega) was used to detect restored luciferase activity to quantify the EVs fused with the recipient cells. A549-LgBiT cells (9×10^4 cells/well) were seeded into a 24-well plate (Iwaki) in DMEM LG containing 10% FBS and incubated at 37 °C with 5% CO_2 for 1 day. The cells were washed twice with 500 μL of PBS(−) and treated with the isolated EVs in DMEM LG containing 10% exosome-depleted FBS for 24 h. The cells were then washed twice with 500 μL of PBS(−) to remove the EVs from the exterior of the cells and trypsinized with 100 μL of 0.01% trypsin in PBS(−)at 37 °C with 5% CO_2 for 10 min. After adding 100 μL of DMEM LG containing 10% FBS, the cells were collected on ice in a 1.5 mL tube. The cells were precipitated by centrifugation (800 × *g*, 4 °C, 5 min), and the supernatant was removed. The cells were resuspended in 50 μL of Opti-MEM. The cells were mixed with 50 μL of a live cell assay reagent containing the substrate in a 96-well optical bottom white plate (Thermo Scientific Nunc), and the luminescence intensity (counts per second) was measured at 25 °C using a Nivo plate reader with an integration time of 1 s per well. The luminescence intensity in live cell buffer (L) was converted to the luminescence intensity in HiBiT lytic detergent buffer (L') using the correction factor (0.72 as mentioned above) between two conditions (eq.1).

$$\boldsymbol{L' = 0.72 \times L\ (eq.1)}$$

The quantity of EVs fused with the recipient cells was determined using the lytic assay calibration curve.

Statistical analysis

Unless specified otherwise, all data were presented as the mean ± standard deviation (SD) of three independent biological experiments (n = 3). Statistical analyses were performed using JMP Pro 15 software (JMP 15.1.0). The calculated *P*-values are shown in the figure legends and are considered significant when $P < 0.05$.

References

(1) Kalluri, R.; LeBleu, V. S. The biology, function, and biomedical applications of exosomes. *Science* **2020**, *367* (6478), eaau6977.
(2) O'Brien, K.; Breyne, K.; Ughetto, S.; Laurent, L. C.; Breakefield, X. O. RNA delivery by extracellular vesicles in mammalian cells and its applications. *Nat. Rev. Mol. Cell Biol.* **2020**, *21* (10), 585-606.
(3) Jiang, J.; Mei, J.; Ma, Y.; Jiang, S.; Zhang, J.; Yi, S.; Feng, C.; Liu, Y.; Liu, Y. Tumor hijacks macrophages and microbiota through extracellular vesicles. *Exploration* **2022**, *2* (1).
(4) Li, M.; Fang, F.; Sun, M.; Zhang, Y.; Hu, M.; Zhang, J. Extracellular vesicles as bioactive nanotherapeutics: An emerging paradigm for regenerative medicine. *Theranostics* **2022**, *12* (11), 4879-4903.
(5) Herrmann, I. K.; Wood, M. J. A.; Fuhrmann, G. Extracellular vesicles as a next-generation drug delivery platform. *Nat. Nanotechnol.* **2021**, *16* (7), 748-759.
(6) Bonsergent, E.; Grisard, E.; Buchrieser, J.; Schwartz, O.; Thery, C.; Lavieu, G. Quantitative characterization of extracellular vesicle uptake and content delivery within mammalian cells. *Nat. Commun.* **2021**, *12* (1), 1864.
(7) Zomer, A.; Maynard, C.; Verweij, F. J.; Kamermans, A.; Schafer, R.; Beerling, E.; Schiffelers, R. M.; de Wit, E.; Berenguer, J.; Ellenbroek, S. I. J. *et al.* In Vivo imaging reveals extracellular vesicle-mediated phenocopying of metastatic behavior. *Cell* **2015**, *161* (5), 1046-1057.
(8) Somiya, M.; Kuroda, S. Real-Time Luminescence Assay for Cytoplasmic Cargo Delivery of Extracellular Vesicles. *Anal. Chem.* **2021**, *93* (13), 5612-5620.
(9) Somiya, M.; Kuroda, S. Reporter gene assay for membrane fusion of extracellular vesicles. *J. Extracell. Vesicles* **2021**, *10* (13), e12171.
(10) van Niel, G.; D'Angelo, G.; Raposo, G. Shedding light on the cell biology of extracellular vesicles. *Nat. Rev. Mol. Cell Biol.* **2018**, *19* (4), 213-228.

(11) Nakase, I.; Futaki, S. Combined treatment with a pH-sensitive fusogenic peptide and cationic lipids achieves enhanced cytosolic delivery of exosomes. *Sci Rep* **2015**, *5*, 10112.
(12) Hikita, T.; Miyata, M.; Watanabe, R.; Oneyama, C. Sensitive and rapid quantification of exosomes by fusing luciferase to exosome marker proteins. *Sci Rep* **2018**, *8* (1), 14035.
(13) Murphy, D. E.; de Jong, O. G.; Evers, M. J. W.; Nurazizah, M.; Schiffelers, R. M.; Vader, P. Natural or Synthetic RNA Delivery: A Stoichiometric Comparison of Extracellular Vesicles and Synthetic Nanoparticles. *Nano Lett* **2021**, *21* (4), 1888-1895.
(14) Joshi, B. S.; de Beer, M. A.; Giepmans, B. N. G.; Zuhorn, I. S. Endocytosis of Extracellular Vesicles and Release of Their Cargo from Endosomes. *ACS Nano* **2020**, *14* (4), 4444-4455.
(15) Dixon, A. S.; Schwinn, M. K.; Hall, M. P.; Zimmerman, K.; Otto, P.; Lubben, T. H.; Butler, B. L.; Binkowski, B. F.; Machleidt, T.; Kirkland, T. A. *et al.* NanoLuc Complementation Reporter Optimized for Accurate Measurement of Protein Interactions in Cells. *ACS Chem. Biol.* **2016**, *11* (2), 400-408.
(16) Kojima, R.; Bojar, D.; Rizzi, G.; Hamri, G. C. E.; El-Baba, M. D.; Saxena, P.; Auslander, S.; Tan, K. R.; Fussenegger, M. Designer exosomes produced by implanted cells intracerebrally deliver therapeutic cargo for Parkinson's disease treatment. *Nat. Commun.* **2018**, *9*, 1305.
(17) Cashikar, A. G.; Hanson, P. I. A cell-based assay for CD63-containing extracellular vesicles. *Plos One* **2019**, *14* (7), e0220007.
(18) Rayamajhi, S.; Aryal, S. Surface functionalization strategies of extracellular vesicles. *J. Mater. Chem. B* **2020**, *8* (21), 4552-4569.
(19) Sung, B. H.; von Lersner, A.; Guerrero, J.; Krystofiak, E. S.; Inman, D.; Pelletier, R.; Zijlstra, A.; Ponik, S. M.; Weaver, A. M. A live cell reporter of exosome secretion and uptake reveals pathfinding behavior of migrating cells. *Nat. Commun.* **2020**, *11* (1), 2092.
(20) Gupta, D.; Liang, X. M.; Pavlova, S.; Wiklander, O. P. B.; Corso, G.; Zhao, Y.; Saher, O.; Bost, J.; Zickler, A. M.; Piffko, A. *et al.* Quantification of extracellular vesicles in vitro and in vivo using sensitive bioluminescence imaging. *J. Extracell. Vesicles* **2020**, *9* (1), 1800222.
(21) Sasaki, M.; Anindita, P. D.; Phongphaew, W.; Carr, M.; Kobayashi, S.; Orba, Y.; Sawa, H. Development of a rapid and quantitative method for the analysis of viral entry and release using a NanoLuc luciferase complementation assay. *Virus Res.* **2018**, *243*, 69-74.
(22) Cocucci, E.; Meldolesi, J. Ectosomes and exosomes: shedding the confusion between extracellular vesicles. *Trends Cell Biol.* **2015**, *25* (6), 364-372.
(23) Cocucci, E.; Meldolesi, J. Ectosomes. *Curr. Biol.* **2011**, *21* (23), R940-941.
(24) Kowal, J.; Arras, G.; Colombo, M.; Jouve, M.; Morath, J. P.; Primdal-Bengtson, B.; Dingli, F.; Loew, D.; Tkach, M.; Théry, C. Proteomic comparison defines novel markers to characterize heterogeneous populations of extracellular vesicle subtypes. *Proc. Natl. Acad. Sci. USA* **2016**, *113* (8), E968-977.
(25) Nakai, W.; Yoshida, T.; Diez, D.; Miyatake, Y.; Nishibu, T.; Imawaka, N.; Naruse, K.; Sadamura, Y.; Hanayama, R. A novel affinity-based method for the isolation of highly purified extracellular vesicles. *Sci. Rep.* **2016**, *6*, 33935.
(26) Kugeratski, F. G.; Hodge, K.; Lilla, S.; McAndrews, K. M.; Zhou, X. N.; Hwang, R. F.; Zanivan, S.; Kalluri, R. Quantitative proteomics identifies the core proteome of exosomes with syntenin-1 as the highest abundant protein and a putative universal biomarker. *Nat. Cell Biol.* **2021**, *23* (6), 631-641.
(27) Jeppesen, D. K.; Fenix, A. M.; Franklin, J. L.; Higginbotham, J. N.; Zhang, Q.; Zimmerman, L. J.; Liebler, D. C.; Ping, J.; Liu, Q.; Evans, R. *et al.* Reassessment of Exosome Composition. *Cell* **2019**, *177* (2), 428-445.

(28) Tian, T.; Zhu, Y. L.; Zhou, Y. Y.; Liang, G. F.; Wang, Y. Y.; Hu, F. H.; Xiao, Z. D. Exosome uptake through clathrin-mediated endocytosis and macropinocytosis and mediating miR-21 delivery. *J Biol Chem* **2014**, *289* (32), 22258-22267.
(29) Schwinn, M. K.; Machleidt, T.; Zimmerman, K.; Eggers, C. T.; Dixon, A. S.; Hurst, R.; Hall, M. P.; Encell, L. P.; Binkowski, B. F.; Wood, K. V. CRISPR-Mediated Tagging of Endogenous Proteins with a Luminescent Peptide. *ACS Chem. Biol.* **2018**, *13* (2), 467-474.
(30) Quinonez, R.; Sutton, R. E. Lentiviral vectors for gene delivery into cells. *DNA Cell Biol.* **2002**, *21* (12), 937-951.
(31) Di Bonito, P.; Ridolfi, B.; Columba-Cabezas, S.; Giovannelli, A.; Chiozzini, C.; Manfredi, F.; Anticoli, S.; Arenaccio, C.; Federico, M. HPV-E7 delivered by engineered exosomes elicits a protective CD8(+) T cell-mediated immune response. *Viruses* **2015**, *7* (3), 1079-1099.
(32) Tominaga, N.; Kosaka, N.; Ono, M.; Katsuda, T.; Yoshioka, Y.; Tamura, K.; Lotvall, J.; Nakagama, H.; Ochiya, T. Brain metastatic cancer cells release microRNA-181c-containing extracellular vesicles capable of destructing blood-brain barrier. *Nat. Commun.* **2015**, *6*, 6716.
(33) Ying, W.; Riopel, M.; Bandyopadhyay, G.; Dong, Y.; Birmingham, A.; Seo, J. B.; Ofrecio, J. M.; Wollam, J.; Hernandez-Carretero, A.; Fu, W. *et al.* Adipose Tissue Macrophage-Derived Exosomal miRNAs Can Modulate In Vivo and In Vitro Insulin Sensitivity. *Cell* **2017**, *171* (2), 372-384 e312.
(34) Nguyen, M. A.; Karunakaran, D.; Geoffrion, M.; Cheng, H. S.; Tandoc, K.; Perisic Matic, L.; Hedin, U.; Maegdefessel, L.; Fish, J. E.; Rayner, K. J. Extracellular Vesicles Secreted by Atherogenic Macrophages Transfer MicroRNA to Inhibit Cell Migration. *Arterioscler Thromb. Vasc. Biol.* **2018**, *38* (1), 49-63.
(35) Uenaka, M.; Yamashita, E.; Kikuta, J.; Morimoto, A.; Ao, T.; Mizuno, H.; Furuya, M.; Hasegawa, T.; Tsukazaki, H.; Sudo, T. *et al.* Osteoblast-derived vesicles induce a switch from bone-formation to bone-resorption in vivo. *Nat. Commun.* **2022**, *13* (1), 1066.
(36) Soares, A. R.; Martins-Marques, T.; Ribeiro-Rodrigues, T.; Ferreira, J. V.; Catarino, S.; Pinho, M. J.; Zuzarte, M.; Isabel Anjo, S.; Manadas, B.; J, P. G. S. *et al.* Gap junctional protein Cx43 is involved in the communication between extracellular vesicles and mammalian cells. *Sci. Rep.* **2015**, *5*, 13243.
(37) Morisaki, T.; Lyon, K.; DeLuca, K. F.; DeLuca, J. G.; English, B. P.; Zhang, Z.; Lavis, L. D.; Grimm, J. B.; Viswanathan, S.; Looger, L. L. *et al.* Real-time quantification of single RNA translation dynamics in living cells. *Science* **2016**, *352* (6292), 1425-1429.

Table of Contents Graphic

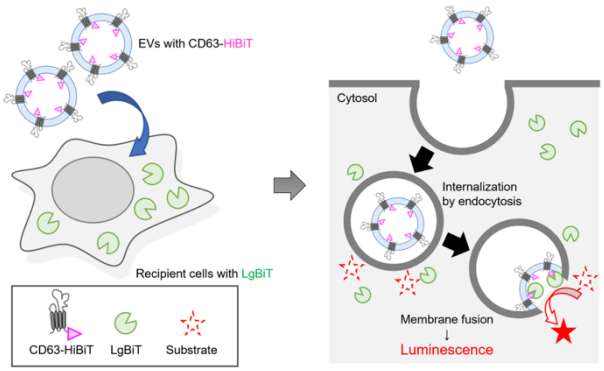

Author Contributions

H.H. designed and directed research, performed experiments, analyzed data and wrote the original manuscript. Y.H. performed most experiments and analyzed data. M.S. and H.S. established A549 cells stably expressing LgBiT. S.F. supervised the project and wrote the manuscript with H.H. All authors commented on the manuscript.

Conflicts of interest

There are no conflicts to declare.

Quantitative analysis of extracellular vesicle uptake and fusion with recipient cells

Hisaaki Hirose,[§]* Yusuke Hirai,[§] Michihito Sasaki,[‡] Hirofumi Sawa,[‡] Shiroh Futaki[†]*

[†]Institute for Chemical Research, Kyoto University, Uji, Kyoto 611-0011, Japan.

[‡]Division of Molecular Pathobiology, International Institute for Zoonosis Control, Hokkaido University, Sapporo, Hokkaido 001-0020, Japan

*Corresponding Authors

E-mail: hirose.hisaaki.5m@kyoto-u.ac.jp, futaki@scl.kyoto-u.ac.jp

Supporting Information

Nanoparticle tracking analysis of EVs

Western blot

Table S1-S2

Figures S1-S5

Nanoparticle tracking analysis of EVs

The number and size of EVs were determined by NTA system using a NanoSight NS300 instrument (Malvern, Worcestershire, UK). The Brownian motion of the sEVs and lEVs was captured at camera levels 16 and 14, respectively, for 1 min (five times) and subsequently analyzed using NTA software (NTA Version: NTA 3.4 Build 3.4.4) with a detection threshold of 4.

Western blot

EVs containing the desired amount of protein were isolated and mixed with sodium dodecyl sulfate (SDS) sample buffer, which did not contain any reducing agents, such as 2-mercaptoethanol. The boiled samples were loaded onto a polyacrylamide gel (SuperSep Ace, 5%–20%, 13 well; FUJIFILM Wako Pure Chemical Corporation) and separated by SDS-polyacrylamide gel electrophoresis (SDS-PAGE). As seen in Fig. S2, SDS-PAGE was performed on 5 μg of cell lysates, 1.5×10^8 particles (Fig. S2A), or 15 μL of isolated sEVs and lEVs (of 100 μL in total volume) (Fig. S2B and S2C). Proteins were transferred onto a polyvinylidene difluoride (PVDF) membrane using Trans-Blot Turbo Transfer System (Bio-Rad, Hercules, CA, USA). The membrane was blocked with 5% BSA in TBS containing 0.05% Tween-20 (TBST) for 1 h at 20-25 °C and then incubated

overnight at 4 °C with appropriate primary antibodies in 5% BSA in TBST. The membrane was incubated with specific horseradish peroxidase (HRP)-conjugated secondary antibodies in 5% BSA in TBST for 1 h at 20-25 °C, followed by washing with TBST three times for 10 min each. Chemiluminescence was detected using ECL prime (Cytiva, Tokyo, Japan) and LAS3000 mini (FUJIFILM).

Table S1. The oligonucleotides used in this study.

Primer / Oligo name	Sequence (5´ → 3´)
HiBiT_Fw	AATTCGGTGGATCAGGAGGAGGTAGTGTTAGTGGATGG AGACTATTCAAGAAGATCTCGTGAGGGCC
HiBiT_Rv	CTCACGAGATCTTCTTGAATAGTCTCCATCCACTAACA CTACCTCCTCCTGATCCACCACCG
VSV-G_Fw	TGACGACAAGTAACTCAAATCCTGCACAACAGATTC
VSV-G_Rv	CCTTATAGTCCTTTCCAAGTCGGTTCATC
FLAG_Fw	AGATGAACCGACTTGGAAAGGACTATAAGGACGATGAC GACAAGTAACTCAAATCCTGCACAAC
FLAG_Rv	GTTGTGCAGGATTTGAGTTACTTGTCGTCATCGTCCTT ATAGTCCTTTCCAAGTCGGTTCATCT
HiBiT_Fw	GGTGGATCAGGAGGAGGTAG
HiBiT_Rv	GGTGGCAAGCTTAAGTTTAAACGC
Halo Tag_Fw	AGCGTTTAAACTTAAGCTTGCCACCATGAGAGGATCGC ATCACCATCAC
Halo Tag_Rv	TAACACTACCTCCTCCTGATCCACCACCGGAAATCTCG AGCGTCG

Table S2. The antibodies used in this study.

Primary antibody	company	Cat. #	dilution ratio
Anti-CD63	FUJIFILM Wako	012-27063	1:1,000
Anti-CD9	Invitrogen	10626D	1:500
Anti-Syntenin	abcam	ab133267	1:1,000
Anti-Annexine A1	abcam	ab214486	1:2,000
Anti-FLAG	Sigma-Aldrich	F3165	1:400
Secondary antibody with HRP	**company**	**Cat. #**	**dilution ratio**
Anti-mouse IgG	Cytiva	NA931	1:5,000
Anti-rabbit IgG	Cell Signaling Tech.	7074	1:1,000

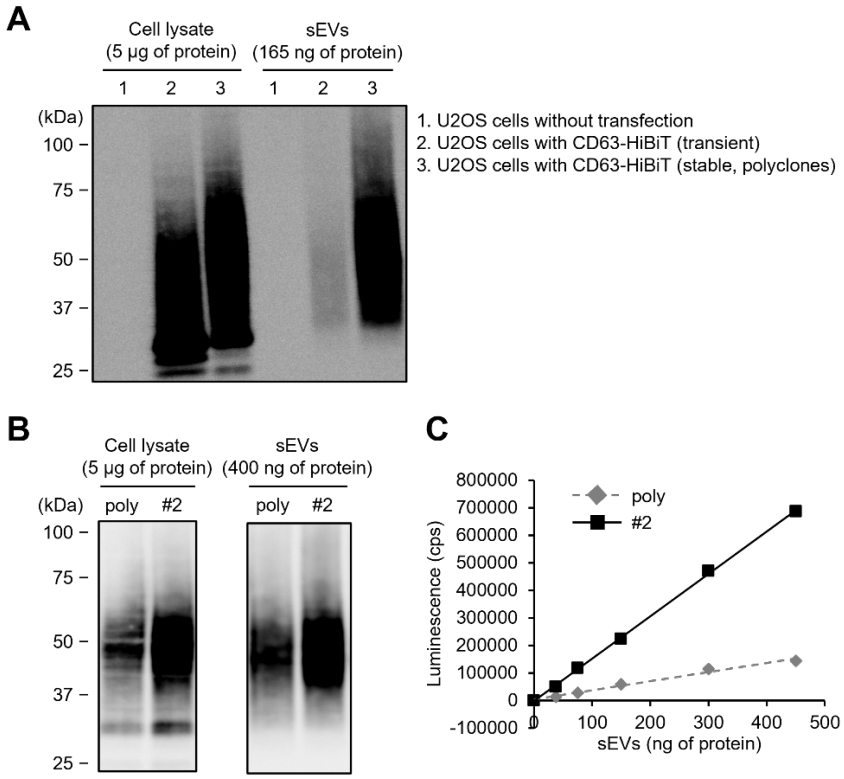

Fig S1. Establishment of U2OS cells stably expressing CD63-HiBiT. (**A**) HiBiT detection of cell lysates and small extracelluar vesicles (sEVs). Lane 1, U2OS cells without transfection; lane 2, U2OS cells transfected with CD63-HiBiT (transient expression); lane 3, U2OS cells stably expressing CD63-HiBiT (polyclones). (**B**) HiBiT detection of cell lysates and sEVs derived from CD63-HiBiT polyclones (poly) and an isolated single clone (#2). (**C**) Standard curves showing the relationship between luminescence and protein amount (ng) of sEVs derived from U2OS-CD63-HiBiT polyclones and the single clone #2.

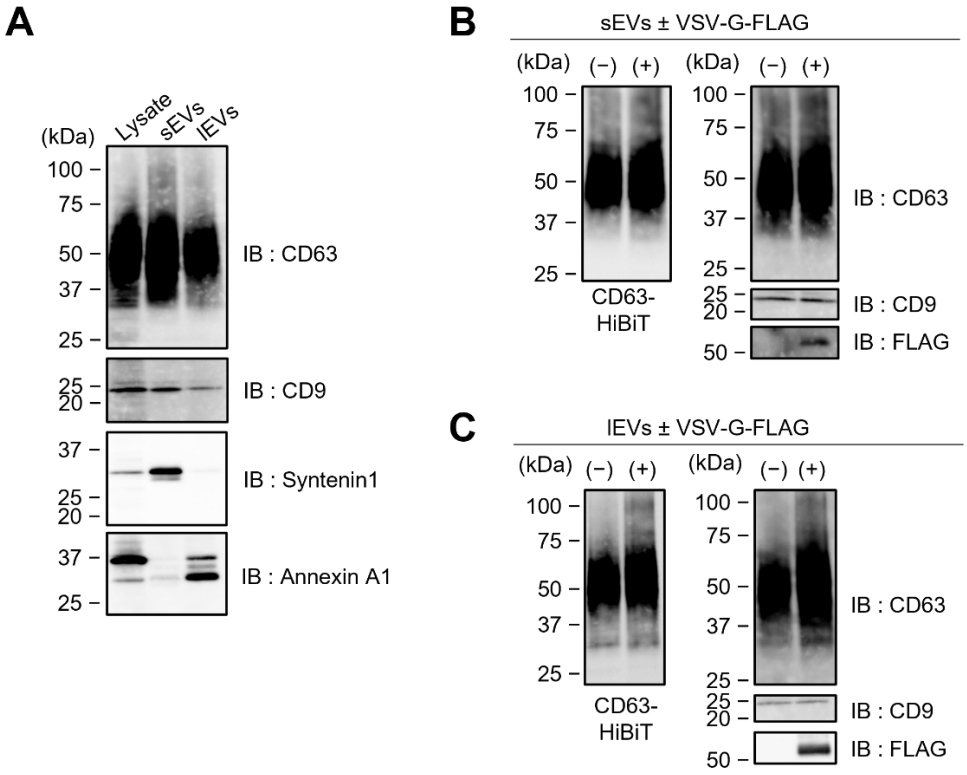

Fig S2. Isolation and characterization of EVs. (**A**) Western blot analysis of EV markers, CD63, CD9, Syntenin1 and Annexin A1. Cell lysates, sEVs, and lEVs derived from U2OS-CD63-HiBiT cells were analyzed. (**B**) HiBiT detection and western blot analysis of sEVs with or without transient expression of VSV-G-FLAG. One representative image is shown. (**C**) HiBiT detection and western blot analysis of lEVs with or without transient expression of VSV-G-FLAG. Representative images of at least two independent experiments are shown. EVs, extracellular vesicles; sEVs, small extracellular vesicles; lEVs, large extracellular vesicles.

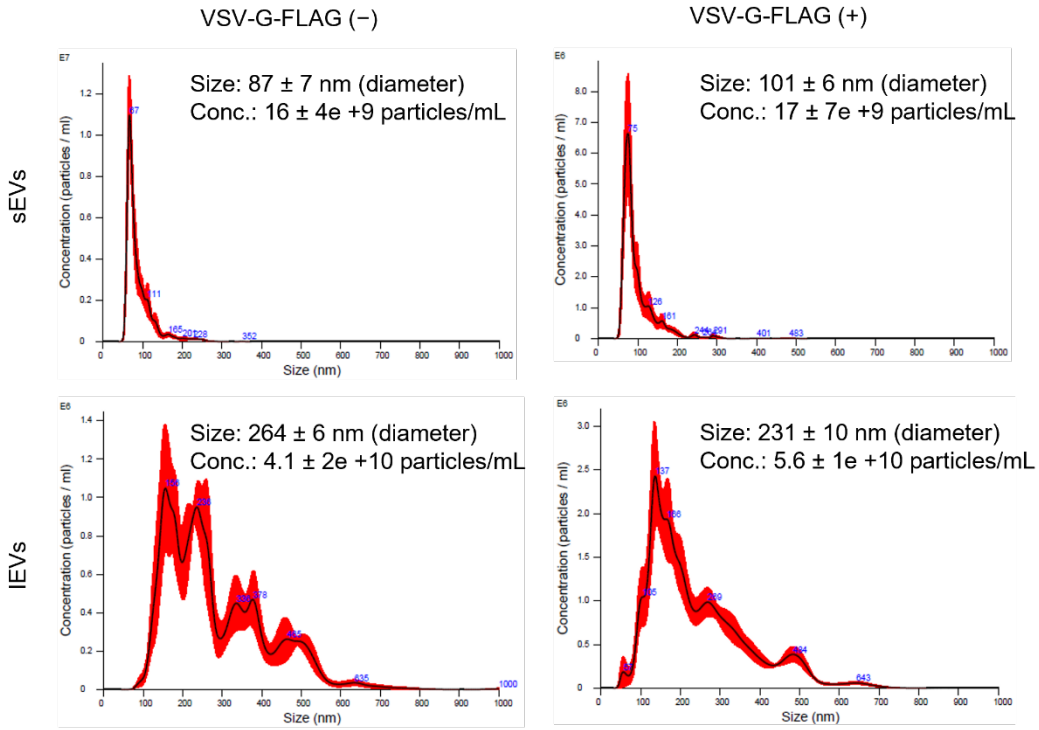

Fig S3. Nanoparticle tracking analysis of sEVs and lEVs derived from U2OS-CD63-HiBiT with or without transient expression of VSV-G-FLAG. The representative data of three independent experiments are shown. The EV sizes and concentrations are shown as mean ± standard deviation (SD) (n = 3). EVs, extracellular vesicles; sEVs, small extracellular vesicles; lEVs, large extracellular vesicles.

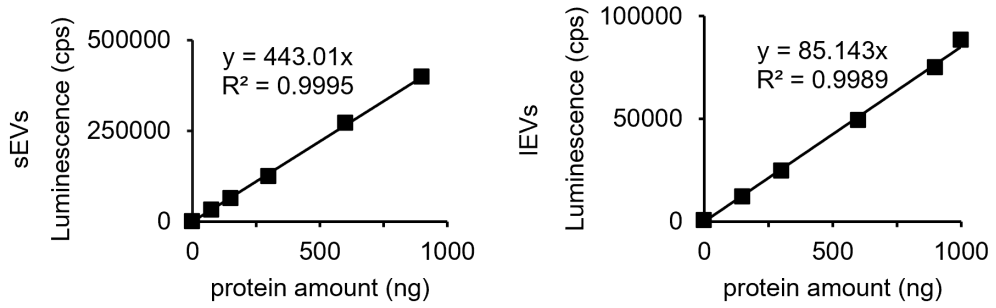

Fig. S4. The relationship between luminscence and total protein amount of small extracellular vesicles (sEVs) and large extracellular vesicles (lEVs). The representative standard curve of three independent experiments presented in Fig. 2 is shown here.

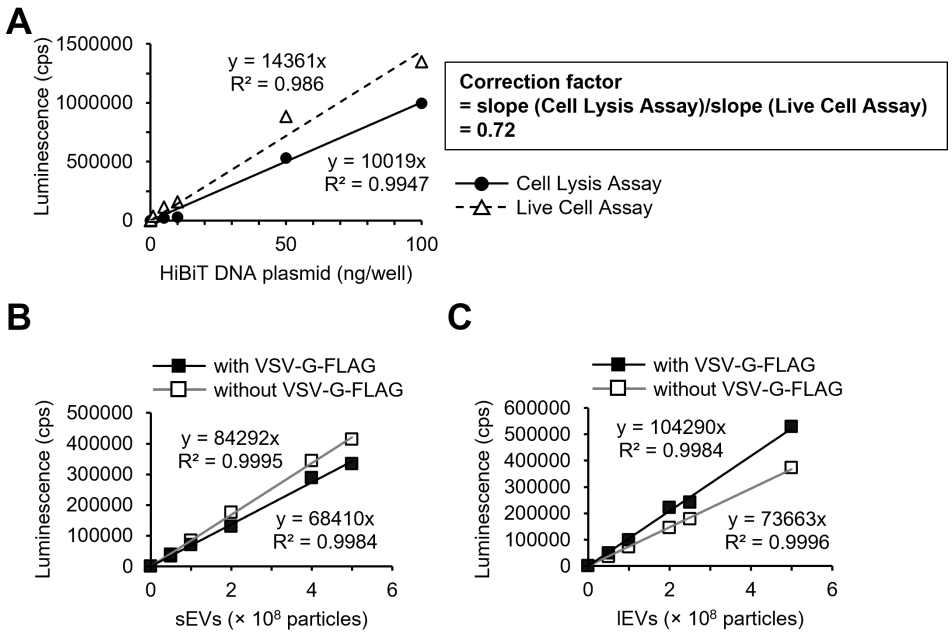

Fig. S5. A correction factor for the live cell assay and the relationship between luminescence and the number of sEVs and lEVs. (**A**) Determination of a correction factor between cell lysis assay and live cell assay. The standard curves between the transfection amount (ng/well) of HaloTag-HiBiT plasmid and its luminescence in the cell lysis assay and live cell assay are shown. One representative graph of three independent experiments is shown. The average of the correction factor of three independent experiments is 0.72. (B, C) The representative standard curve between luminescence and the number of sEVs and lEVs of three independent experiments in Table 2 is shown. sEVs, small extracellular vesicles; lEVs, large extracellular vesicles.